

Supporting Information File

Tuning dimensionality between 2D and 1D MOFs by lanthanide contraction and ligand-to-metal ratio.

Fernando González Chávez^{*[1]} and *Hiram Isaac Beltrán*^{*[2]}

1) *Posgrado en Ciencias Naturales e Ingeniería, UAM Cuajimalpa, 05300, Ciudad de México, México;*

2) *Departamento de Ciencias Básicas, DCBI, UAM Azcapotzalco, 02200, Ciudad de México, México.*

Table of contents

Figure S1. Powder X-ray diffraction patterns of PBIA-Er _{2D} simulated, PBIA-Er _{2D} experimental, PBIA-Tm _{2D} experimental, and PBIA-Pr _{2D} experimental.....	2
Figure S2. FTIR spectra of Pr, Tm and Er 2D materials.	2
Figure S3. Thermograms of PBIA-Pr _{2D} , PBIA-Tm _{2D} , and PBIA-Er _{2D}	3
Figure S4. H-bonding interactions between 1D chains in PBIA-Tm _{1D}	4
Table S1. Selected geometrical parameters of PBIA-Tm _{1D}	5
Figure S5. Simulated PXRD pattern of PBIA-Tm _{1D} and experimental patterns of PBIA-Tm _{1D} and PBIA-Er _{1D}	6
Figure S6. FTIR spectra of PBIA-Tm _{1D}	6
Figure S7. FTIR spectra of PBIA-Er _{1D}	7

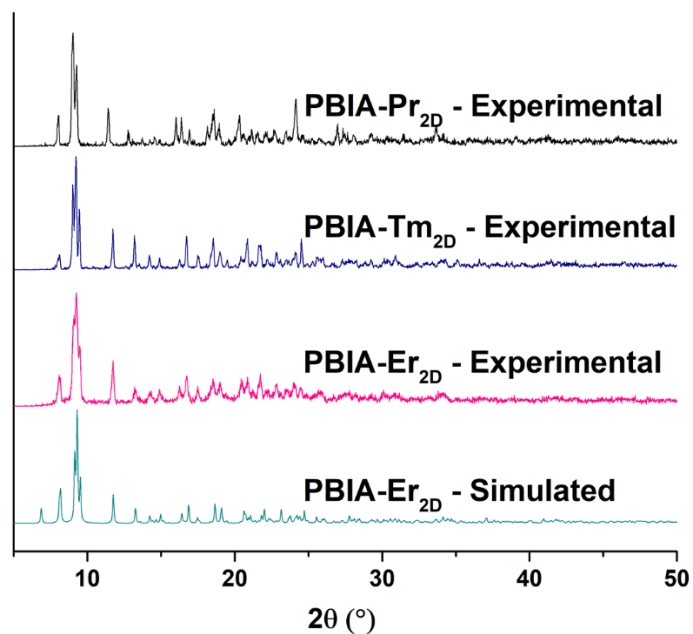


Figure S1. Powder X-ray diffraction patterns of PBIA-Er_{2D} simulated (light blue), PBIA-Er_{2D} experimental (pink), PBIA-Tm_{2D} experimental (blue), and PBIA-Pr_{2D} experimental (black). These compounds are isostructural, thus, experimental patterns are compared with the simulated powder pattern from the SCXRD of PBIA-Er_{2D}.

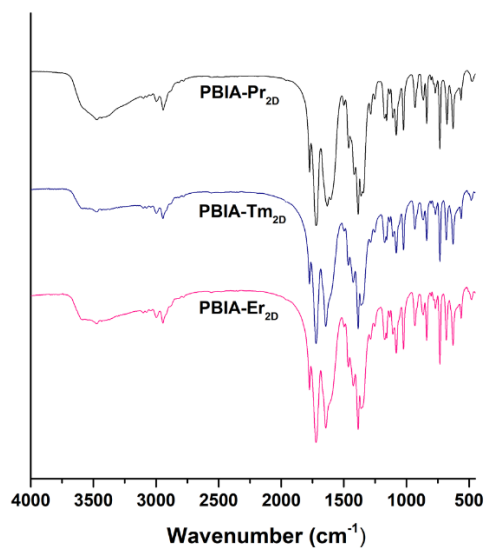


Figure S2. FTIR spectra of Pr, Tm and Er 2D materials.

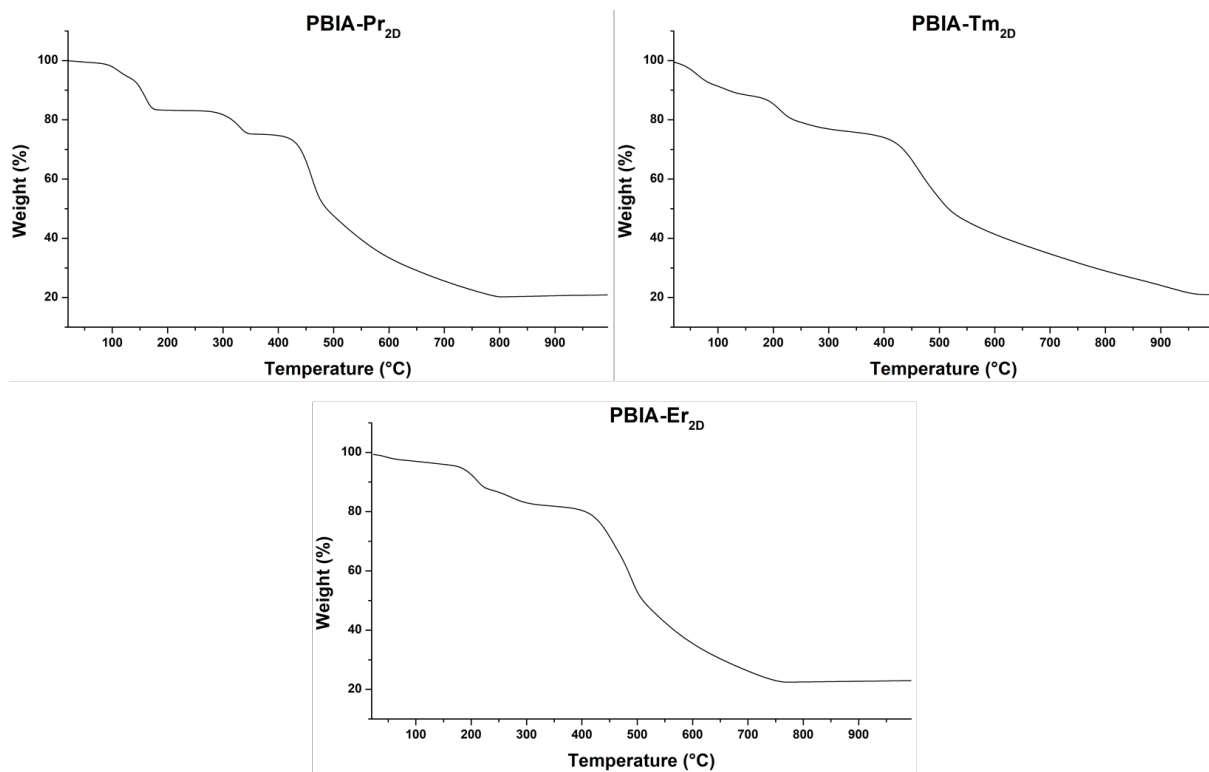


Figure S3. Thermograms of PBIA-Pr_{2D}, PBIA-Tm_{2D}, and PBIA-Er_{2D}.

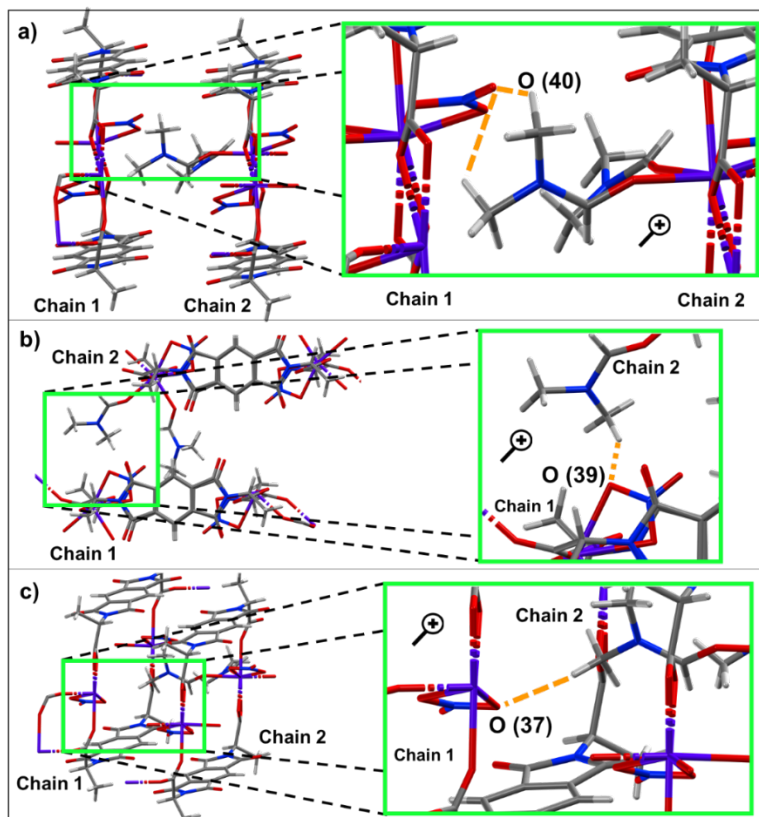


Figure S4. H-bonding interactions between 1D chains in PBIA-Tm₁₀. Interactions between a) O(40), b) O(39), and c) O(37) from nitrate with hydrogens from DMF of the adjacent chain.

Table S1. Selected geometrical parameters of PBIa-Tm₁₀

Bond distances [Å]	PBIa-Tm₁₀
Tm-O(1) _{iso}	2.2584(18)
Tm-O(26) _{iso}	2.2433(17)
Tm-O(18) _{bidentate-chelate}	2.354(2)
Tm-O(19) _{bidentate-chelate}	2.409(2)
Tm-O(37) _{bidentate-nitrate}	2.457(2)
Tm-O(39) _{bidentate-nitrate}	2.375(2)
Tm-O(27) _{DMF1}	2.261(9)
Tm-O(27A) _{DMF1A}	2.230(5)
Tm-O(32) _{DMF2}	2.266(7)
Tm-O(32A) _{DMF2A}	2.285(6)
C(2)-O(26)	1.235(3)
C(2)-O(1)	1.237(3)
C(17)-O(18)	1.241(4)
C(17)-O(19)	1.233(4)
N(38)-O(37)	1.258(5)
N(38)-O(39)	1.270(4)
N(38)-O(40)	1.219(4)
C(28)-O(27)	1.155(11)
C(28A)-O(27A)	1.116(12)
C(33)-O(32)	1.243(9)
C(33A)-O(32A)	1.321(10)
Bond angles [°]	
O(26)-Tm-O(1) _{iso}	89.09(7)
O(18)-Tm-O(19) _{bidentate-chelate}	53.95(8)
O(37)-Tm-O(39) _{bidentate-nitrate}	52.89(10)
O(1)-C(2)-O(26) _{iso}	126.4(2)
O(18)-C(17)-O(19) _{bidentate-chelate}	121.7(3)
O(37)-N(38)-O(39) _{bidentate-nitrate}	116.8(3)
Dihedral angles [°]	
Tm-O(26)-C(2)-O(1)	-85.7(4)
Tm-O(1)-C(2)-O(26)	14.9(6)
C(2)-O(1)-Tm-O(26)	16.5460(13)
C(2)-O(26)-Tm-O(1)	76.157(2)
Tm-O(19)-C(17)-O(18)	3.4(4)
Tm-O(18)-C(17)-O(19)	-3.5(4)
Tm-O(37)-N(38)-O(1)	3.32760(2)
Tm-O(39)-N(38)-O(37)	-3.4636(2)

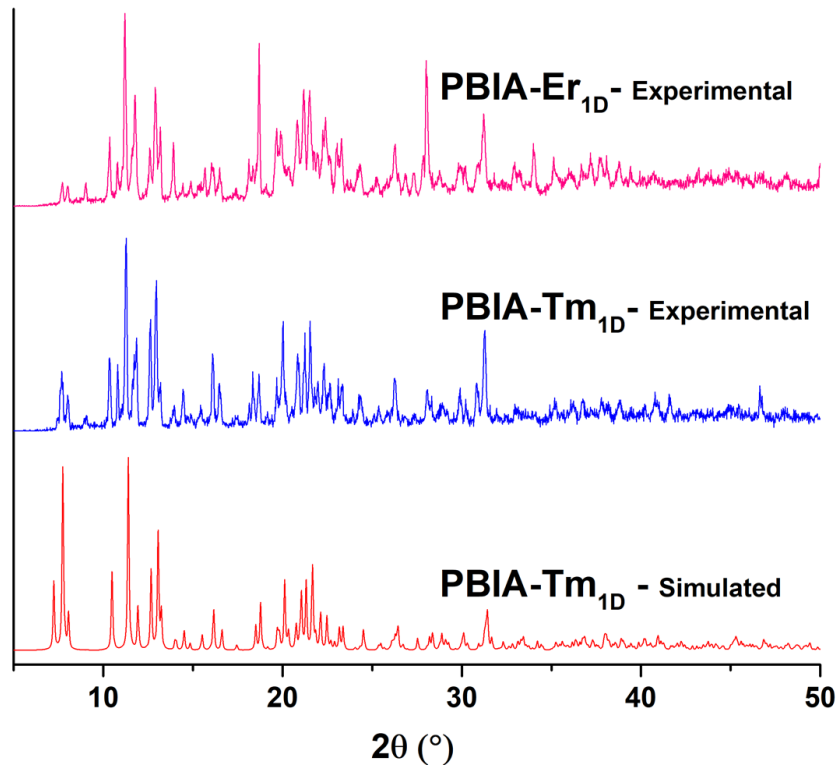


Figure S5. Simulated PXRD pattern of PBIA-Tm_{1D} (red). Good agreement is observed among experimental patterns of PBIA-Tm_{1D} (blue) and PBIA-Er_{1D} (pink).

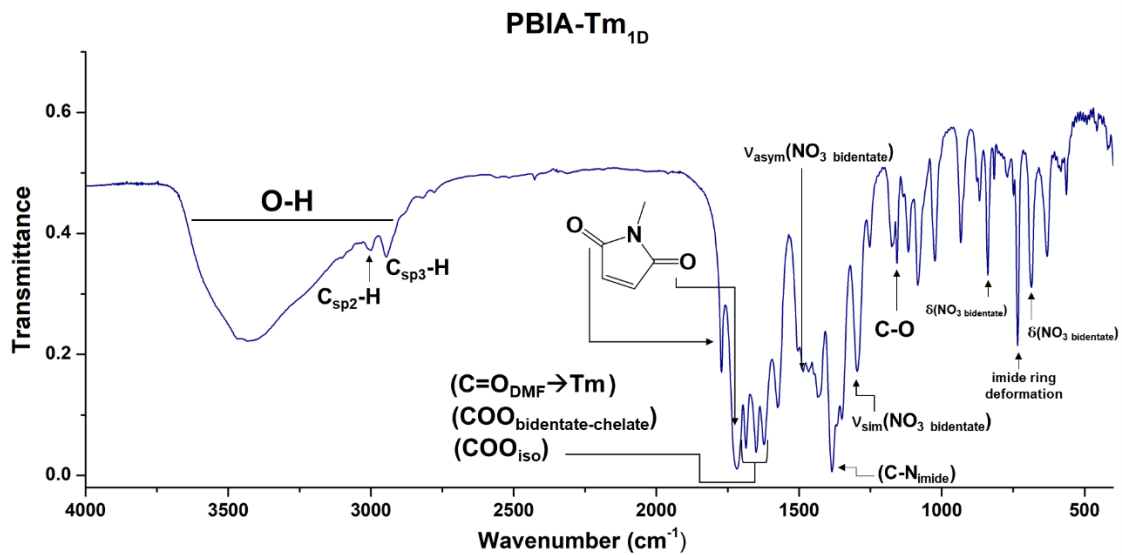


Figure S6. FTIR spectra of PBIA-Tm_{1D}.

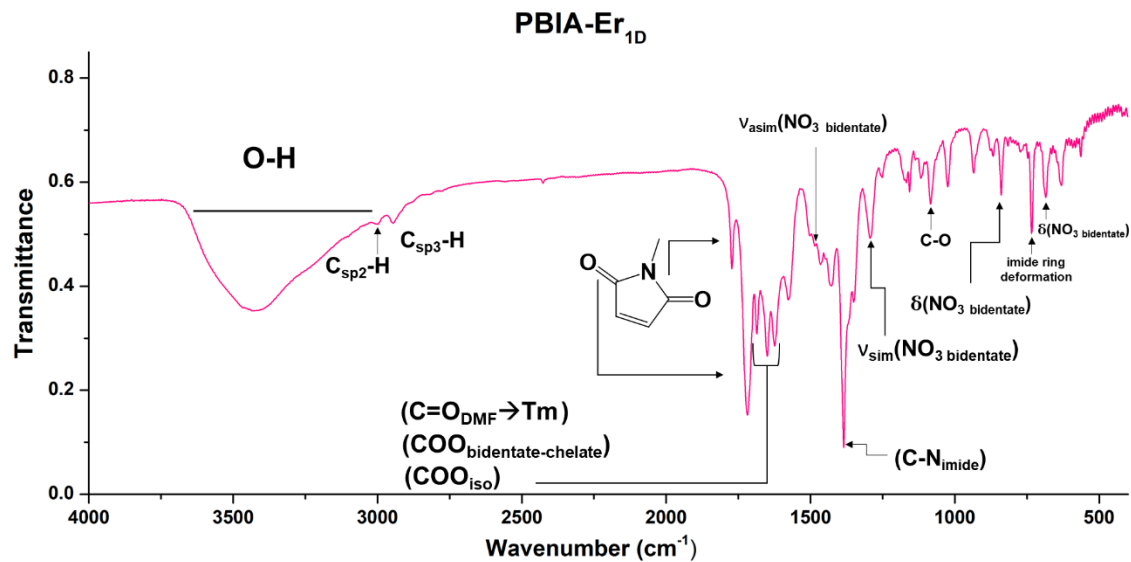


Figure S7. FTIR spectra of PBIA-Er_{1D}.